Local Bond Stress-Slip Model for R/C Joints and Anchorages with Moderate Confinement

Lotfi Guizani [a, *], Omar Chaallal [a, 1], Seyed Sina Mousavi [a, 2]

[a] Department of Construction Engineering, University of Quebec, École de technologie supérieure, 1100 Notre-Dame West, Montreal QC, Canada.

* Corresponding author, Tel.: +1 514-396-8420, E-mail address: lotfi.guizani@etsmtl.ca

[1] E-mail address: omar.chaallal@etsmtl.ca

[2] E-mail address: seyedsina.m@gmail.com

Authors' accepted manuscript of the article published in
Canadian Journal of Civil Engineering, vol. 44 no 3, pp. 201-211
http://dx.doi.org/10.1139/cjce-2015-0333

Abstract: This paper presents a summary of an experimental investigation and the derivation of a bond-slip model for reinforcing steel embedded in moderately confined concrete under monotonic and cyclic loadings. Moderately confined concrete encompasses the domain between unconfined and well-confined concrete, the limits of which are defined in the paper. The proposed constitutive law adapts and extends the well-known Eligehausen-Filippou law for well-confined concrete to moderately confined concrete. It is described by an envelope curve and degradation rules. The former is obtained through a confinement index, defined in this study as a function of the amount of confining steel and concrete, distance between confining steel and the rebar and concrete segregation effect. It is proposed to adopt the same degradation rules used for well-confined concrete. These rules are validated through statistical tests for moderately confined concrete. They are found to predict correctly the main features of reduced envelope response under increasing cycling amplitudes but to underestimate response degradation under constant cycling limits for the subsequent cycles to the first cycle. To demonstrate the validity and limitations of the proposed model, its predictions under monotonic loading are compared with experimental results and analytical predictions from other studies.

Keywords: bond, slip, concrete, confinement index, monotonic loading, cyclic loading, splitting crack.

Introduction

In locations of moderate to strong seismic activities, reinforced concrete (RC) structures are typically designed to undergo deformations well beyond their elastic range without substantial loss of strength and stiffness. Inelastic deformations are however concentrated in so-called plastic zones of limited dimensions within the structure. These plastic zones are the main seismic energy-dissipating mechanisms in the event of an earthquake and govern the overall performance of the structure. Therefore, the ability of models used to capture their hysteretic behaviour is of paramount importance to obtain reliable results for dynamic analyses. Under seismic forces, the plastic zones are generally subjected to excessive cracking due to accumulated damage under repeated cycles. A factor contributing to crack opening is the slip of the main reinforcing bars at their anchorage and within RC joints (Brown and Jirsa 1971; Popov 1984; Limkatanyu and Spacone 2003; Lobo and Almeida 2015). This slip, which is either neglected or roughly approximated in most nonlinear analysis models, results in fixed-end rotations that lead to additional deformations and additional displacements of the structure (Filippou et al. 1983, 1986; Saatcioglu et al. 1992; Mitra and Lowes 2007; Lobo and Almeida 2015).

A complete review of bond-slip mechanisms associated to reinforcing steel bars in concrete may be found in Goto (1971), Tassios (1979) and Eligehausen et al. (1983). Bond failure is governed by two extreme modes characterizing well-confined and unconfined concrete, respectively: (1) Pull-out failure, after shearing of the concrete surrounding the reinforcing steel bar and; (2) Splitting failure of the concrete surrounding the bar which slips easily, by wedging, after rapid propagation and opening of the splitting crack. The pull-out mode yields the maximum possible bond resistance, as a function of the resistance of concrete around the bar. In contrast, splitting failure mode is associated to very low resistance in absence of adequate confinement to restrain propagation and opening of the splitting cracks. Between these two extreme modes span intermediate modes of failure combining a partial shearing of the concrete around the bar with a controlled splitting crack opening and propagation. These modes are associated with moderately confined concrete, subject of this study.

Splitting of concrete around a pulled out reinforcing bar is initiated at an early stage as a result of the formation of a radial hoop stress inherent to the load transfer, by contact pressure, between

inclined deformed bar lugs and the surrounding concrete. If the restraint against the radial stress, so called confinement action, is strong and stiff enough, then splitting cracks will be limited to the immediate zone around the reinforcing bar and their opening will remain very small. On the other hand, if the confinement action is weak and/or insufficient, the main splitting crack will propagate to reach the faces of the structure and its opening continues to increase with slip. After splitting, the bond-slip behaviour is thereby very sensitive to the confining conditions of the concrete and the restraint against the splitting crack opening. At this stage, all factors affecting the resistance to hoop stress are determinant to bond-slip response. Presence of restraint against opening of the splitting crack, such as steel intercepting the splitting crack plan or a confining pressure are found among the most important factors affecting bond-slip behaviour after splitting (Gambarova et al. 1989a, b; Giuriani et al. 1991; Gambarova and Rosati 1996; Plizzari et al. 1996; Plizzari et al. 1998; Harajli et al. 2004; Guizani and Chaallal 2011).

The importance of studying the bond-slip behaviour for moderately confined concrete is justified by the fact that in many practical situations, steel-reinforcement slip may originate from zones of moderately confined concrete as defined earlier. This is often the case for splice zones and old structures designed with less stringent seismic provisions as well as for transitions areas between unconfined and well-confined concrete in ductile structures (Harajli et al. 2004). Furthermore, old structures, especially those exposed to de-icing salts in north climates, such as parking structures and bridges, are prone to important degradation and cracking of their concrete cover combined to steel corrosion. Stirrups, which are usually located at the outer layers of concrete, are particularly exposed to severe corrosion and reduction of their section at an earlier age than the main reinforcing bars (Sajedi and Huang 2015; Zhou et al. 2015). Such section reduction of stirrups, combined with concrete cover deterioration, greatly affects the confining conditions of the concrete and hence bond-slip behaviour of the main reinforcement, which would frequently fall within the domain of the moderately confined concrete studied in this paper.

The bond stress-slip law for well-confined concrete is soundly established. The original bond-slip law proposed by Eligehausen et al. (1983), or its slightly modified version used by Filippou et al. (1983), hereafter called Eligehausen-Filippou model, have been widely and successfully used for numerical simulations of bond-slip within well-confined critical regions under

generalized loadings, such as ductile RC frame joints (Filippou et al. 1983; Russo et al. 1990; Monti et al. 1997; Monti and Spacone 2000; Limkatanyu and Spacone 2003). It was also adopted by the CEB-FIP Model Code 90 (CEB-FIP 1993) and was used as a base model for many bond-slip laws extended to simulate the behaviour in Polymer Fiber Reinforced concrete (Rossetti et al. 1995; Cosenza et al. 1997; Lin and Zhang 2014). On the other hand, bond-slip behaviour of beam splices, typically controlled by splitting of concrete cover, has been extensively studied under monotonic and cyclic loadings and many bond-slip laws were developed (Orangun et al. 1977; Giuriani 1981; Gambarova et al. 1989a; Giuriani et al. 1991; Gambarova and Rosati 1996; Rezansoff et al. 1997; Esfahani and Rangan 1998; Harajli et al. 2004; Harajli 2006; Harajli 2009). Nevertheless, bond-slip relations reported in the literature for concrete controlled by splitting cracking are limited to specific situations such as beam splices, under monotonic loading or under cyclic loading, but with limited slip amplitudes. For example, Harajli et al. (2004) presented a local bond model under monotonic loading for unconfined and moderately confined concrete with steel, fiber and polymer jackets. This model was generalized later to cyclic loading in Harajli (2009). However, this model, while covering a wide range of applications and featuring a very good agreement with experimental observations, is based on half cycle tests representing stress conditions that prevail at typical spliced reinforcing bars in zones of beams under dominant flexure. Therefore, these models for splices do not represent moderately confined concrete within interior joints where stress and cracking state is different and where considerable cyclic slippage can occur in both directions. The existing bond-laws for concrete controlled by splitting suffer serious shortcomings for use in seismic analyses of some critical regions such as joints or anchorage regions with moderately confined concrete, governed by splitting cracks, under generalized full reversal large amplitude cycling. The development of a bond stress-slip law under generalized loadings, representative of joints with moderate confining conditions is still needed to undertake reliable evaluation of the performance of many structures such as existing old and deteriorated structures.

The main objective of this paper is to present a bond stress-slip constitutive law developed for moderately confined concrete under generalized cyclic loading. The proposed law is based on an extensive experimental investigation and is aiming to extend the widely used Eligehausen-Filippou bond-slip law for the well-confined concrete under generalized cycling loading to the

moderately confined concrete of joints and anchorages. A summary of the experimental programme and its main findings are presented in this paper. Further details can be found in Guizani and Chaallal (2011).

Experimental Programme

Factors Investigated

Forty-three (43) pull-out specimens with 25M reinforcing bars, embedded in concrete on a short distance of $5d_b$, were tested under monotonic and cyclic loadings (Guizani and Chaallal 2011). Specimens were designed to represent confining conditions representative of moderately confined concrete within reinforced concrete joints and/or anchorage regions, governed by splitting crack propagation. Six (06) factors were considered in the experimental study that can be grouped into two categories. Four (04) factors, related to physical concrete-confinement conditions (see Fig. 1) were studied by the monotonic loading tests (M-Series) and two (02) factors related to cyclic history were studied in the cyclic loading tests (C-Series). The M-Series factors are:

1) The quantity of steel confining the bonded area, represented by a non-dimensional steel-index, *S*, defined as the ratio of confining-steel area (A_{cs}) to the area of the tested rebar in the plane of the splitting crack ($A_{bs}= l\, d_b$). That is:

$$S = \frac{A_{cs}}{l d_b} \quad (1)$$

Where, l is the anchorage length and d_b is the tested (pulled-out) bar diameter.

2) The quantity of concrete confining the bonded area, represented by a non-dimensional concrete-confinement index, *C*. This factor represents the bar spacing, S_b, and/or concrete cover (Fig. 1). It is defined as the ratio of the confining concrete area, $A_{cc}= l(S_b - d_b)$, to the area of the tested rebar in the plane of the splitting crack, $A_{bs}= l d_b$. Its expression simplifies to Eq. (2):

$$C = \frac{S_b}{d_b} - 1 \quad (2)$$

3) The distance (center-to-center) between the tested rebar and the confining steel, *d*. This factor is represented by the factor *D*, defined as the ratio of *d* to the diameter of the tested rebar, d_b. That is:

(3) $$D = \frac{d}{d_b}$$

4) The height of the concrete cast below the tested rebar, *h*. This factor, described by a non-dimensional index *H*, represents fresh-concrete segregation effect on bond, also known as ″top bar effect″. It is defined as:

(4) $$H = \frac{h}{d_b}$$

The cyclic series (C-Series) runs were carried out at average values of the above described M-Series four factors and aimed to study the effect of the loading history on bond degradation. Each run consisted of applying N_c initial cycles of a slip amplitude A_c, followed by three large cycles of 30 mm (±15 mm) slip amplitude. The 5th and 6th factors, studied by C-Series and their possible values are:

5) The number of initial cycles: N_c =1.0 or 10;
6) The slip amplitude of the initial cycles: A_c =±0.05, ±0.25, ±0.5, ±2.0 or ±8.0mm.

The thirty (30) monotonic (M-Series) and thirteen (13) cyclic(C-Series) pull out tests are presented in Tables 1 and 2, respectively. Physical values of confining steel area A_{cs}, bar spacing S_b, distance *d* and height of fresh concrete below the bar, *h* can be obtained using equations (1) to (4) with d_b=25.4 mm and *l*=127 mm (5d_b). The M-Series consisted of a central composite design with a duplicated fractional 2^{4-1} experimental plan (Montgomery 2008). Extreme values (star points) of *S, C, D and H* factors were chosen to match as close as possible the boundaries of the studied domain and to cover a wide range of practical values. Details regarding test specimens, properties of used materials and test procedures can be found in Guizani and Chaallal (2011).

Response Parametrisation and Response Variables

Examination of the obtained bond-slip response curves under monotonic loading suggested that the bond-slip response envelope curve is well represented by a modified shape of the Eligehausen et al. (1983) bond-slip envelope curve, widely adopted for the well-confined concrete, as shown in Fig. 2.

The modified curve is defined by seven parameters, namely s_1, s_2, s_3, τ_1, τ_3, and α, used for the response curve of well-confined concrete plus an additional seventh parameter, τ_2, which represents the bond stress at the characteristic slip s_2 (Guizani and Chaallal 2011). This added characteristic stress, τ_2, was adopted to reflect the observed drop in bond strength, after concrete splitting. Such drop was observed to have a variable importance depending on the available confining steel that can be mobilised to hold the tensile stress liberated by the splitting of concrete. To evaluate the effect of the studied factors on the bond-slip response under monotonic loading, for each run, the proposed model was fit, as close as possible, to the obtained experimental response envelope and the values of the seven parameters mentioned above and providing such a fit are considered as experimental values. These values were then defined as the response variables (RV), used for statistical analysis to determine the influencing factors on monotonic bond response. In addition to these seven RV, the characteristic energy absorbed by the bond mechanism, E_0, was also computed and considered for the statistical analysis. The characteristic energy E_0 is defined as the area below the observed response curve between the origin and the characteristic slip, s_3 as shown in Fig. 2. A low energy value is associated with a brittle bond failure (e.g., unconfined concrete), while a high energy value results from a ductile bond failure (e.g., confined concrete). This is a particularly important parameter in the Eligehausen-Filippou model since the degradation of bond under cycling is defined in terms of a damage index, D, calculated as the ratio of the cumulated dissipated energy under cycling to the characteristic energy E_0 (Eligehausen et al. 1983).

Experimental Results: Summary and Analysis

A number of mechanisms and basic rules related to the behaviour of bond and the load transfer between the steel reinforcement and concrete in moderately confined concrete can be pointed out from the experimental study carried out by the authors and from earlier studies (e.g., Eligehausen et al. 1983; Giuriani et al. 1991; Plizzari et al. 1996; Harajli et al. 2004; Oh and Kim 2007; Harajli 2009).

All the forty three (43) tested specimens showed a complete propagation of a discrete splitting crack, along a predefined weak plane, up to their external faces. Before the occurrence of such a splitting crack, tested specimens showed a bond response similar to that of well-confined

concrete. The splitting-crack propagation was accompanied by a transfer of the radial forces from the concrete to the confining steel. If the quantity of confining steel was not sufficient to resist the transferred radial forces following complete concrete splitting, then the splitting crack continued to open rapidly and an abrupt reduction of the bond stress was observed. Such a situation resulted in a fragile type of behaviour where the greater was the deficit in confining steel, the more markedly the resistance decreased after splitting and the smaller was the residual frictional resistance (Guizani and Chaallal 2011). This type of behaviour is characterized by a low value of the characteristic energy E_0. In contrast, if the quantity of confining steel provided was sufficient to support the transferred force from splitting concrete, then the crack opening remained small and progressed slowly while the bond resistance continued to increase with increasing slip, reaching a maximum resistance at the yielding of the confining steel. Thereafter, the response entered a descending phase where the bond resistance steadily and gradually decreased as the imposed slip increased. The response reached a residual frictional resistance at an imposed slip value around the clear distance between the bar lugs. This residual resistance increased with the quantity of confining steel, and its maximum value corresponds to the residual strength of well-confined concrete. For greater slips, the bond residual resistance remained practically constant (Guizani and Chaallal 2011).

Table 3 presents the experimental values for the seven parameters defining the bond-slip response under monotonic loading, obtained by the best fitting process explained earlier. In addition, the characteristic energy, E_0 and the maximum splitting crack opening, w_{max}, are listed for each run. As shown later, the characteristic slip s_2 is found independent of the studied parameters and have a value around 3.0 mm, as for well-confined concrete. Thus, the value of bond stress at 3.0 mm, noted as τ'_2 is listed in table 3 and is used later for the proposed model and the presented regressions for τ_2.

Fig. 3 shows typical obtained experimental cyclic bond-slip responses from the C-Series runs and a schematic representation of the cyclic response. Examination of the obtained cyclic responses features reveals that the reduced envelopes, the unloading and reloading branches as well as the residual frictional resistance follow the same trends as those observed for the well-

confined concrete reported and extensively explained in Eligehausen et al. (1983) (Guizani and Chaallal 2011).

The experimental degradation indices (parameters) were measured and compared to the prediction of the Eligehausen-Filippou model through statistical tests of the null hypothesis (Guizani and Chaallal 2011). The statically tested parameters are those measuring the degradation of the response under cycling and were grouped into three classes: 1) parameters related to the reduced envelope curve after one (1) or many cycles; 2) parameters related to degradation of the response under constant cycling within the cycling interval and; 3) parameters measuring the degradation of the residual frictional resistance.

Statistical test results indicate that, independently of the number of cycles and as long as the maximum imposed slip do not go beyond the characteristic slip s3, the reduced envelope curves are very fairly predicted by the Eligehausen-Filippou model degradation rules. However, these rules underestimate the degradation of reduced envelope for the 2^{nd} and subsequent cycles within the cycling slip interval as well as the degradation of the friction resistance for large amplitude cycling.

Derivation of Generalised Cyclic Bond-Slip Law

Based on the above experimental results and their analysis and on further regression analysis presented below, a bond-slip law under generalised cycling is developed in the following. The bond law consists of a primary or envelope curve describing the behaviour under monotonic loading and a set of degradation rules describing the response under cycling. The following sections present the derivation and the computation of the proposed bond-slip law features.

Model and Parameters for the Envelope Curve

The proposed model for the primary curve of bond-slip is shown in Fig. 2. It is described by four (04) branches defined by seven characteristic parameters (τ_1, τ_2, τ_3, s_1, s_2, s_3 and α) as expressed in Eq. (5):

$$(5) \qquad \begin{cases} \tau = (s/s_1)^{\alpha}\tau_1 & for \quad 0 \le s \le s_1 \\ \tau = \tau_1 - (\tau_1 - \tau_2)(s - s_1)/(s_2 - s_1) & for \quad s_1 \le s \le s_2 \\ \tau = \tau_2 - (\tau_2 - \tau_3)(s - s_2)/(s_3 - s_2) & for \quad s_2 \le s \le s_3 \\ \tau = \tau_3 & for \quad s \ge s_3 \end{cases}$$

The determination of the seven parameters, defining the envelope response under monotonic loading, of Eq. (5), as a function of concrete confining conditions, is presented in below.

Representation of Concrete Confinement Conditions into a Confinement Index

For a more general representation, the studied four factors related to the concrete confining conditions are recast into a unique factor called the confinement index, I_c. The use of this index is more rational than purely empirical approaches and is more consistent with the analytical modelling and theory of bond behaviour governed by the splitting cracks progression (e.g., Giuriani et al. 1991; Plizzari et al. 1996; Plizzari et al. 1998; Harajli et al. 2004; Harajli 2009). Such an index, I_c, is a global indicator of the total confinement force which is available to resist the propagation and opening of the splitting crack and which can be mobilized by both the confining steel and the confining concrete. In this study, the confining index, I_c, is computed as follows:

$$(6) \qquad I_c = S f(D) + \frac{C f(H)}{n}$$

The terms *S*, *C*, *D,* and *H* are the observed values of the four factors defined in Eqs. (1) to (4). The terms *f(D)* and *f(H)* are weighting functions for factors *S* and *C* to take into account the effects of factors *D* and *H* respectively. Parameter *n* is a positive real number, which translates the strength of the confining concrete to its equivalent in confining steel.

By expressing the effects of factors *D* and *H* as weighting functions of factors *S* and *C* respectively, the intrinsic link between these factors is accounted for. For example, the effect of factor *D* depends on the magnitude of factor *S* and disappears as the latter tends towards zero. Consequently, it is appropriate to choose a weighting function *f(D)* tending towards zero when the factor *D* tends towards infinity to reflect the diminishing influence of the confining steel with increasing distance to the reinforcing bar.

The weighting functions *f(D)* and *f(H)* and the denominator *n* have been chosen such that the correlation between the confinement index, I_c, and E_0 is maximized. The resulting function *f(D)* is given by the following:

$$f(D) = \begin{cases} 1.0 & if\ D \le 2.0 \\ 1 - (\frac{D}{D_{cr}})^2 & if\ 2.0 \le D \le D_{cr} \\ 0.0 & if\ D \ge D_{cr} \end{cases} \quad (7)$$

Where D_{cr} represents a critical distance beyond which the quantity of confining steel has no significant effect on the local bond response. From experimental results, it has been established that this critical distance depends on the quantity of confining steel (S) and can be approximated as follows:

$$D_{cr} = 4 + 300S - 3800S^2 \ge 4.0 \quad (8)$$

Concrete segregation is known to affect the mechanical properties of concrete, in particular compression, tension, shear, and bond strengths. The function *f(H)* had been chosen to be in the exponential form, as follows:

$$f(H) = (a + bH)^p \quad (9)$$

The coefficients a, b, and p were determined iteratively so that the coefficient of variation, R^2, of the regression equation relating the confinement index, I_c, (Eq. (5)) to E_0 was maximized. This iterative process led to an optimal value of p of approximately 0.5. The proposed expression is therefore:

$$f(H) = \sqrt{1.067 - 0.0167H} \quad (10)$$

Equation (10) confirms earlier studies that established that bond resistance in well-confined concrete is proportional to the square root of the concrete compressive strength (Eligehausen et al. 1983; Harajli et al. 2004; Harajli 2009).

The confining force that can originate from concrete after the complete propagation of a splitting crack is attributable to its residual resistance in tension, and is substantially smaller than that

observed before crack propagation. The proposed model captures this difference by means of the term n, expressed as follows:

$$n = 1000 - 50C \tag{11}$$

Thus, if there is enough concrete to prevent the propagation of the splitting crack, then the concrete contribution is at its maximum. This corresponds to a small value of n ($\leq$350, within the range of steel's yield stress, f_y, to the concrete's modulus of rupture, f_r: f_y/f_r). By contrast, if the concrete alone cannot prevent the propagation of the splitting crack (small value of C), the concrete's contribution becomes marginal. This corresponds to a large value of n ($\approx$1000, within the range of $f_y/(0.1f_r)$).

Calculation of the Characteristic Energy E_0

As discussed earlier, the characteristic energy E_0 is the response variable (RV) that best describes the overall behaviour of bond. This variable, illustrated in Fig. 2, is related to the energy dissipated by bond and distinguishes between fragile and ductile types of behaviour. Therefore, to obtain a more generalized constitutive model, it was deemed convenient to relate the characteristic energy ratio E_0 to the global confinement index, I_c. Furthermore, examination of the experimental results reveals that the variables defining the response envelope are strongly correlated to E_0. Therefore, simple but accurate and coherent regression relations are proposed for predicting the envelope response parameters in terms of the E_0, instead of the studied factors. It follows that the proposed model is based on regression equations, which not only take into account the experimental results of this study, but are also consistent with the existing body of theoretical and experimental knowledge on bond behaviour. Finally, in order for the proposed model to encompass different concrete conditions (such as concrete strength, ribs geometry, bars diameter), it is proposed to use a normalized ratio E_0/E_c instead of an absolute value of E_0. The normalization term used, E_c, is the absorbed energy under the envelope response, up to a slip equal to s_3, for well- confined concrete. A theoretical value of E_c=153.5 N/mm, based on the Eligehausen-Filippou model for well-confined concrete, and considering the tested concrete strength (42.7MPa) and the geometry of bar ribs of the tested specimens (s_3=12.3mm) was obtained.

The E_0/E_c ratio is correlated to the confinement index I_c by the following regression equation (R^2=0.88, Fig. 4):

(12a) $$0.0 \le E_0/E_c = 0.0327+60.3I_c-2576\ I_c^2+40158\ I_c^3 \le 0.8 \quad \text{for } I_c \le 0.0378.$$

As shown in Fig. 4, this relation offers an excellent correlation with experimental values for I_c ranging from 0.0 to 0.0378. The latter value is practically equal to the maximum I_c value of 0.0373 obtained for the undertaken tests. The proposed equation (12a) is found subject to multicollinearity with high Variance Inflation Factors (VIF) that is induced by including high order terms. We assessed the validity of the regression by standardising the data (centring on the mean value of I_c=0.01825) in order to reduce multicollinearity and preventing it from hiding significant terms (Minitab 2014, Shacham and Brauner 1997). By doing so, the VIF considerably reduced (from above 100 to fewer than 8.4). Also, all terms of the regression, except the I_c term, are found statistically significant with p-values not above 0.002. The term I_c is however included in the regression as its p-Value is 5.6%, which is very close to the 5% usual acceptance level. The Standard Error (SE) of the regression equation 12a) is 0.0625, which is considered low. Residuals do not show any particular trend with a distribution similar to a random normal distribution.

The proposed regression is valid for the I_c ranging from 0.0 and 0.0378. However, earlier studies have shown that the lower limit for the confining index associated with well-confined concrete is around 0.004 to 0.005 (Plizzari et al. 1996; Plizzari et al. 1998). Goto (1971) found that the angle β, that is, the angle between the axis of rebar and the reaction of the bar lug against concrete, varies between 45° and 80°. Given this angle β, the radial force can be obtained, and hence the required confinement index to prevent splitting. Such value defines the lower limit of the well-well confined concrete domain and varies approximately between 0.035 for β=45° and 0.15 for β=80°. A reasonable estimate of the minimum confinement index to qualify as well-confined concrete would be I_c=0.07, which corresponds to a β value of approximately 60°. Therefore, as shown in Fig. 4, a linear interpolation between 0.8 at I_c=0.0378 and 1.0 at I_c=0.07 is assumed to calculate E_0/E_c, which leads to the following equation:

(12b) $$0.8 < E_0/E_c = 6.21\ I_c+0.565 \le 1.0 \quad \text{for } 0.0378< I_c \le 0.07.$$

Determination of the Envelope Curve Parameters

The E_0/E_c ratio is a key parameter for deriving the proposed model. It is obtained from equations (12a) or (12b), as a function of the only confinement index, *Ic*, representing the local confining conditions of the concrete under consideration, established by equations (6) to (11). Once the E_0/E_c ratio is obtained, all the parameters defining the bond envelope curve for moderately confined concrete are derived, as indicated below, in function of this ratio and the maximum and residual bond resistances of well-confined concrete. These resistances, as well as the characteristic energy E_c, may be obtained beforehand as per Eligehausen et al. (1983) or the CEB-FIP (1993) models.

Statistical analysis of the obtained experimental results, presented in Guizani and Chaallal (2011), have shown that similarly to well-confined concrete, for moderately concrete, the characteristic slips s_2 and s_3 are also independent of the confining conditions (index). That is:

(13) $$s_2 = 3.0\,mm$$

(14) $$s_3 = \text{Clear spacing between bar ribs}$$

The parameter α, defining the nonlinear initial branch is set equal to the average value obtained from M-Series, that is:

(15) $$\alpha = 0.23$$

As shown in Fig. 5, a very strong correlation exists between the ratio of the characteristic resistance τ_2 to the maximum resistance of well-confined concrete, τ_{1c}, and the ratio E_0/E_c. The following regression (R^2=0.90) is proposed:

(16) $$\frac{\tau_2}{\tau_{1c}} = 1.05\frac{E_0}{E_c} \leq 1.0$$

Fig. 6 shows the variation of τ_2/τ_1 ratio with the E_0/E_c ratio. At lower values of the E_0/E_c ratio, τ_2/τ_1 increases rapidly and reaches a value around the unity at a value of E_0/E_c about 0.5 to 0.6, resulting in the following regression equation (R^2=0.754):

(17) $$\tau_2/\tau_1 = 2.477\,(E_0/E_c) - 1.52\,(E_0/E_c)^2 \leq 1.0$$

The above Eq. (17) allows calculation of τ_1 once τ_2 obtained by Eq. (16). For E_0/E_c greater than 0.8, the ratio τ_2/τ_1 is set to the maximum value of 1.0. In addition, Eq. (17) is deemed inadequate for cases with no confining steel combined to an insufficient concrete cover. For such cases, the bond response suddenly decreases to a negligible value after the propagation of the splitting crack. Thus, for S=0 and E_0/E_c less than 0.6, the characteristic value τ_2 should be assumed equal to the residual frictional resistance τ_3. The residual frictional resistance, τ_3, is calculated in terms of the residual resistance of well-confined concrete, τ_{3c}, and the E_0/E_c ratio by the following regression equation (R^2=0.88, Fig. 7):

(18) $$\tau_3/\tau_{3c}=0.96(E_0/E_c)^2 +0.02\ E_0/E_c$$

The characteristic slip, s_1, shows a large scatter. The best obtained correlation of this parameter is obtained with the ratio τ_2/τ_1 (R^2=0.54), as follows:

(19) $$s_1 = 0.07e^{2.94(\tau_2/\tau_1)}$$

As will be shown later, for low confinement levels ($I_c \leq 0.01$) a better prediction of the slip at maximum bond response is obtained using the parameter s_{max} of the model presented by Harajli et al. (2004).

Cyclic Response and Degradation Rules

It is proposed to adopt and extent the use of the degradation rules of the Eligehausen-Filippou model, originally developed for well-confined concrete, for cyclic degradation of bond of moderately confined concrete. As shown earlier, if used with the appropriate envelope curve, as established above for moderately confined concrete, these rules can predict with reasonable accuracy the main features of the cyclic response, notably the reduced envelopes. It should be mentioned that such rules are found to underestimate the degradation of bond resistance for subsequent cycling (beyond the first cycle) within a constant amplitude cycles. Nevertheless, the reduced envelope curve subsequent to such loading is still correctly predicted using the selected rules. Therefore, the overall accuracy of the response is considered satisfactory with a need for proposing a better degradation rules for the response subsequent to the first cycle under constant amplitude cycling and for the residual friction resistance as these responses degrade faster for moderately confined concrete than for well-confined concrete.

Validation of the Proposed Model

The proposed model can be considered to be implicitly validated by the results achieved through the experimental program carried out by the authors, as shown in Figs. 4 to 7 and the coefficient of determination R^2. In addition, the proposed model predicted envelope responses for a selection of tests from the M-Series are plotted in Fig. 8, together with the experimental fitted curves and the predictions of other analytical models, namely the Harajli et al. (2004) and Wu and Zhao (2012) models.

As shown in Fig. 8, the proposed model compares more favourably to experimental results of our studies than all the other considered models. Although Harajli et al. (2004) as well as Wu and Zhao (2012) models predict fairly well the maximum bond resistance, they largely underestimate the post peak branch and particularly the residual frictional resistance. CEB-FIP (1993) models do not predict correctly the observed responses.

Furthermore, Fig. 9 compares the experimental responses reported by Harajli et al. (2004) for a splice specimen to the predictions of the proposed model and to those of Harajli et al. (2004) and Wu and Zhao (2012) models. The proposed model is found to accurately estimate the maximum bond resistance but overestimates the post-peak response. However, generally the maximum response predicted by the proposed the model is higher than the measured bond strength obtained from splice specimens.

It is interesting to note that this corresponds to the inverse picture of the comparison in Fig. 8 of the proposed model predictions and other models predictions for pull-out experimental results. The differences are mainly attributed to the fact that pullout test is not appropriate to represent splice zones as the stress state and crack pattern are different. Similar conclusion was reported by many researchers who reported that pullout tests resulted in higher bond strengths (Tighiouart et al. 1998; ACI 408R-03 2003; Tastani and Pantazopoulou 2009; Cairns 2015). Pullout tests generate an arching action of compression struts that creates an additional confining action of the bonded zone, which increases the bond response particularly in the post-peak response where any contribution to confine and limit the opening of the splitting crack has a major impact. From a basic Strut-and-Tie model of the tested specimens, we computed an additional confining stress of about 30% of the measured bond-stress.

Finally, the predictions of the proposed model are compared, in Fig. 10, with the experimental results obtained for series 1.3 and 1.4 from Eligehausen et al. (1983), which used similar pullout-test specimens. These series are representative of the confining conditions prevailing near the lower and upper boundaries of the studied domain.

As shown, an excellent agreement between the response curve predicted by the proposed model and the experimental curves obtained by Eligehausen et al. (1983) for Series 1.3. For Series 1.4, where no confining steel was provided, a very satisfactory agreement is obtained if the characteristic resistance τ_2 is set equal to τ_3, as recommended earlier for these cases. Without such an adjustment, the model overestimates the post peak response in a similar way as when compared to the splice run B3N, from Harajli et al. (2004), presented in Fig. 9.

Conclusions

This paper presents the derivation of a bond stress-slip constitutive model for moderately confined concrete of RC Joints and anchorage zones under cyclic loading. It is based on experimental results carried out by the authors and summarized in this paper. The model is composed of an envelope curve that describes the bond stress-slip response under monotonic loading, which forms the envelope of the cyclic response, and cyclic rules that describe the loading and unloading phases and the reduced (degraded) envelope curves, as a function of the loading history and the envelope curve. The proposed envelope curve, is a modified version of the widely used curve for well-confined concrete, proposed by Eligehausen et al. (1983), and is derived on basis of a global confining index, defined in the paper and which takes into account the confining conditions of concrete. Cyclic rules of Elighehausen-Filippou model are adopted after their validation through statistical analyses of the obtained experimental response from the cyclic runs. These rules allow a globally very satisfactory prediction of the response, especially after 1 cycle. However, they underestimate the response degradation within constant amplitude subsequent cycling and need a future enhancement. Finally, comparisons of the proposed model predictions with results of earlier research studies and other models demonstrate the accuracy of the proposed model for moderately confined of anchorages and RC joints under monotonic loading. However, they also point out limitation of the proposed model, which overestimates the bond response of spliced zones because of the inherent flaws of the pullout test. Additional testing of the cyclic degradation rules at other low levels of confining is also recommended in order to enhance their formulation and consequently their predictions under generalised seismic loadings.

Acknowledgments

The financial support provided by the Natural Science and Engineering Research Council of Canada (NSERC) is gratefully acknowledged.

References

ACI Committee 408. 2003. Bond and development of straight reinforcing bars in tension, ACI 408R-03.

Brown, R.H. and Jirsa, J.O., 1971, May. Reinforced concrete beams under load reversals. In Journal Proceedings, **68**(5): 380-390. doi:10.14359/11338.

Cairns, J. 2015. Bond and anchorage of embedded steel reinforcement in fib Model Code 2010. Structural Concrete, **16**(1): 45-55. doi:10.1002/suco.201400043.

CEB-FIP. 1993. Comité euro-international du béton, CEB-FIP model code 1990: design code. Telford.

Cosenza, E., Manfredi, G., and Realfonzo, R. 1997. Behavior and modeling of bond of FRP rebars to concrete. Journal of composites for construction, **1**(2): 40-51. doi:10.1061/(asce)1090-0268(1997)1:2(40).

Eligehausen, R., Popov, E.P., and Bertero, V.V. 1983. Local Bond Stress-Slip Relationships of Deformed Bars under Generalized Excitations. EERC report UCB/EERC-83/23, University of California, Berkeley, California, 162 p.

Esfahani, M.R., and Rangan, B.V. 1998. Bond between normal strength and high-strength concrete (HSC) and reinforcing bars in splices in beams. Structural Journal, **95**(3): 272-280. doi:10.14359/545.

Filippou, F.C., Popov, E.P., and Bertero, V.V. 1983. Modeling of R/C joints under cyclic excitations. Journal of Structural Engineering, **109**(11): 2666-2684. doi:10.1061/(asce)0733-9445(1983)109:11(2666).

Filippou, F.C., Popov, E.P., and Bertero, V.V. 1986. Analytical studies of hysteretic behavior of R/C joints. Journal of Structural Engineering, **112**(7): 1605-1622. doi:10.1061/(asce)0733-9445(1986)112:7(1605).

Gambarova, P.G., and Rosati, G. 1996. Bond and splitting in reinforced concrete: test results on bar pull-out. Materials and Structures, **29**(5): 267-276. doi:10.1007/bf02486361.

Gambarova, P.G., Rosati, G.P., and Zasso, B. 1989a. Steel-to-concrete bond after concrete splitting: constitutive laws and interface deterioration. Materials and Structures, **22**(5): 347-356. doi:10.1007/bf02472505.

Gambarova, P.G., Rosati, G.P., and Zasso, B. 1989b. Steel-to-concrete bond after concrete splitting: test results. Materials and Structures, **22**(1): 35-47. doi:10.1007/bf02472693.

Giuriani, E. 1981. Experimental investigation on the bond-slip law of deformed bars in concrete. In IABSE Colloquium Delft 1981, Advanced Mechanics of Reinforced Concrete, Rep. of the Working Commissions. Vol. 34, pp. 121-142.

Giuriani, E., Plizzari, G., and Schumm, C. 1991. Role of stirrups and residual tensile strength of cracked concrete on bond. Journal of Structural Engineering, **117**(1): 1-18. doi:10.1061/(asce)0733-9445(1991)117:1(1).

Goto, Y. 1971, April. Cracks formed in concrete around deformed tension bars. In Journal Proceedings, **68**(4): 244-251. doi:10.14359/11325.

Guizani, L., and Chaallal, O. 2011. An experimental study on bond-slip in moderately confined concrete subjected to monotonic and cyclic loading using an experimental plan. Canadian Journal of Civil Engineering, **38**(3): 272-282. doi:10.1139/l10-133.

Harajli, M. 2009. Bond stress–slip model for steel bars in unconfined or steel, FRC, or FRP confined concrete under cyclic loading. Journal of structural engineering, **135**(5): 509-518. doi:10.1061/(asce)0733-9445(2009)135:5(509).

Harajli, M.H. 2006. Effect of confinement using steel, FRC, or FRP on the bond stress-slip response of steel bars under cyclic loading. Materials and structures, **39**(6): 621-634. doi:10.1007/s11527-005-9054-z.

Harajli, M.H., Hamad, B.S., and Rteil, A.A. 2004. Effect of confinement on bond strength between steel bars and concrete. Structural Journal, **101**(5): 595-603. doi:10.14359/13381.

Limkatanyu, S., and Spacone, E. 2003. Effects of reinforcement slippage on the non-linear response under cyclic loadings of RC frame structures. Earthquake engineering & structural dynamics, **32**(15): 2407-2424. doi:10.1002/eqe.334.

Lin, X., and Zhang, Y. 2014. Evaluation of bond stress-slip models for FRP reinforcing bars in concrete. Composite Structures, **107**: 131-141. doi:10.1016/j.compstruct.2013.07.037.

Lobo, P.S., and Almeida, J. 2015. RC fiber beam–column model with bond-slip in the vicinity of interior joints. Engineering Structures, **96**: 78-87. doi:10.1016/j.engstruct.2015.04.005.

Minitab, I. 2014. MINITAB release 17: statistical software for windows. Minitab Inc, USA.

Mitra, N., and Lowes, L.N. 2007. Evaluation, calibration, and verification of a reinforced concrete beam–column joint model. Journal of Structural Engineering, **133**(1): 105-120. doi:10.1061/(asce)0733-9445(2007)133:1(105).

Montgomery, D.C. 2008. Design and analysis of experiments. John Wiley & Sons.

Monti, G., Filippou, F.C., and Spacone, E. 1997. Finite element for anchored bars under cyclic load reversals. Journal of Structural Engineering, **123**(5): 614-623. doi:10.1061/(asce)0733-9445(1997)123:5(614).

Monti, G., and Spacone, E. 2000. Reinforced concrete fiber beam element with bond-slip. Journal of Structural Engineering, **126**(6): 654-661. doi:10.1061/(asce)0733-9445(2000)126:6(654).

Oh, B.H., and Kim, S.H. 2007. Realistic models for local bond stress-slip of reinforced concrete under repeated loading. Journal of Structural Engineering, **133**(2): 216-224. doi:10.1061/(asce)0733-9445(2007)133:2(216).

Orangun, C., Jirsa, J., and Breen, J. 1977. A reevaulation of test data on development length and splices. In Journal Proceedings, **74**(3): 114-122. doi:10.14359/10993.

Plizzari, G.A., Deldossi, M.A., and Massimo, S. 1998. Transverse reinforcement effects on anchored deformed bars. Magazine of Concrete Research, **50**(2): 161-178. doi:10.1680/macr.1998.50.2.161.

Plizzari, G.A., Marchina, E., and Giuriani, E. 1996. Experimental study of splitting and flexural cracks in a RC beam with overlapped splices. Materials and Structures, **29**(1): 19-27. doi:10.1007/bf02486003.

Popov, E.P. 1984. Bond and anchorage of reinforcing bars under cyclic loading. In Journal Proceedings, **81**(4): 340-349. doi:10.14359/10689.

Rezansoff, T., Zhang, S., and Sparling, B. 1997. Influence of different stirrup configurations on lap splices in beams. Canadian Journal of Civil Engineering **24**(1): 106-114. doi:10.1139/cjce-24-1-106.

Rossetti, V.A., Galeota, D., and Giammatteo, M. 1995. Local bond stress-slip relationships of glass fibre reinforced plastic bars embedded in concrete. Materials and Structures, **28**(6): 340-344. doi:10.1007/BF02473149.

Russo, G., Zingone, G., and Romano, F. 1990. Analytical solution for bond-slip of reinforcing bars in RC joints. Journal of Structural Engineering, **116**(2): 336-355. doi:10.1061/(asce)0733-9445(1990)116:2(336).

Saatcioglu, M., Alsiwat, J.M., and Ozcebe, G. 1992. Hysteretic behavior of anchorage slip in R/C members. Journal of Structural Engineering, **118**(9): 2439-2458. doi:10.1061/(asce)0733-9445(1992)118:9(2439).

Sajedi, S., and Huang, Q. 2015. Probabilistic prediction model for average bond strength at steel–concrete interface considering corrosion effect. Engineering Structures, **99**: 120-131. doi:10.1016/j.engstruct.2015.04.036.

Shacham, M., and Brauner, N. 1997. Minimizing the effects of collinearity in polynomial regression. Industrial & engineering chemistry research, **36**(10): 4405-4412. doi:10.1021/ie970236k.

Tassios, T.P. 1979. Properties of bond between concrete and steel under load cycles idealizing seismic actions. Bulletin d'information du CEB, (131): 65-122.

Tastani, S., and Pantazopoulou, S. 2009. Direct tension pullout bond test: Experimental results. Journal of Structural Engineering, **136**(6): 731-743. doi:10.1061/(asce)st.1943-541x.0000159.

Tighiouart, B., Benmokrane, B., and Gao, D. 1998. Investigation of bond in concrete member with fibre reinforced polymer (FRP) bars. Construction and building materials, **12**(8): 453-462. doi:10.1016/s0950-0618(98)00027-0.

Wu, Y.-F., and Zhao, X.-M. 2012. Unified bond stress–slip model for reinforced concrete. Journal of Structural Engineering, **139**(11): 1951-1962. doi:10.1061/(asce)st.1943-541x.0000747.

Zhou, H., Lu, J., Xv, X., Dong, B., and Xing, F. 2015. Effects of stirrup corrosion on bond–slip performance of reinforcing steel in concrete: An experimental study. Construction and Building Materials, **93**: 257-266. doi:10.1016/j.conbuildmat.2015.05.122.

List of tables

Table 1: Monotonic loading series, (M-Series)

Table 2: Cyclic loading series, (C-Series)

Table 3: Summary of experimental results for monotonic loading series, (M-Series)

Table 1: Monotonic loading series, (M-Series)

Run (ID)	Values of studied factors			
	S	C	D	H
M1.11, M1.12	0.00982	1.00	0.8	3.0
M1.21, M1.22	0.02945	1.00	5.6	3.0
M1.31, M1.32	0.00982	3.00	5.6	3.0
M1.41, M1.42	0.02945	3.00	0.8	3.0
M1.51, M1.52	0.00982	1.00	5.6	19.0
M1.61, M1.62	0.02945	1.00	0.8	19.0
M1.71, M1.72	0.00982	3.00	0.8	19.0
M1.81, M1.82	0.02945	3.00	5.6	19.0
M2.01 to M2.06	0.0196	2.00	3.2	6.0
M2.11, M2.12	0.0000	2.00	3.2	6.0
M2.21, M2.22	0.03927	2.00	3.2	6.0
M2.31, M2.32	0.0196	0.00	3.2	6.0
M2.41, M2.42	0.0196	4.00	3.2	6.0
C-Series of Table 2	0.0196	2.0	3.2	6.0

Table 2: Cyclic loading series, (C-Series)

Amplitude of initial loading cycles (A_c)	Number of initial cycles (N_c)			
	01 cycle		10 cycles	
0.1mm (±0.05 mm)	-----	-----	C-1-10-1	-----
0.5mm (±0.25mm)	C-2-01-1	-----	C-2-10-1	C-2-10-2
1.0mm (±0.5mm)	C-3-01-1	-----	C-3-10-1	C-3-10-2
4.0mm (±2.0mm)	C-4-01-1	C-4-01-2	C-4-10-1	C-4-10-2
16.0mm (±8.0mm)	C-5-01-1	-----	C-5-10-1	-----

Table 3: Summary of experimental results for monotonic loading series, (M-Series)

Test #	τ_1 (MPa)	τ_2 (MPa)	τ_3 (MPa)	τ'_2 (MPa)	s_1 (mm)	s_2 (mm)	s_3 (mm)	α (MPa)	E_0 (N/mm)	w_{max} (mm)
M1.11	12.8	7.7	1.0	6.9	0.4	1.6	13.2	0.38	66.6	1.2
M1.12	7.8	6.6	1.0	5.7	0.4	1.6	13.0	0.2	53.0	2.2
M1.21	13.6	8.4	1.0	7.2	0.06	1.0	13.0	0.25	73.2	1.63
M1.22	10.8	8.0	1.3	7.6	0.1	2.4	13.0	----	75.9	0.35
M1.31	12.6	1.0	0.0	6.7	0.2	3.8	13.0	0.17	32.7	3.2
M1.32	12.1	5.2	0.15	4.9	0.23	2.4	13.0	0.35	47.1	2.75
M1.41	11.8	11.8	3.0	11.4	0.62	3.0	13.0	0.2	105.1	1.1
M1.42	12.6	12.6	3.0	11.4	0.7	3.0	13.0	0.18	108.3	0.57
M1.51	10.0	6.0	1.4	6.9	0.8	3.6	12.8	0.3	60.8	1.1
M1.52	8.3	5.0	0.03	5.0	0.8	3.0	----	0.2	34.4	2.5
M1.61	10.8	10.0	1.8	9.3	0.9	2.0	13.0	0.32	77.9	1.1
M1.62	10.1	10.1	2.4	9.4	1.1	1.9	14.0	0.3	88.3	0.6
M1.71	10.0	6.0	0.75	6.4	0.96	2.5	13.0	0.29	77.9	2.08
M1.72	9.4	6.6	1.1	7.0	0.75	3.6	13.0	0.25	62.3	1.4
M1.81	9.4	9.4	1.9	9.2	1.6	3.2	13.0	0.2	80.1	0.48
M1.82	9.4	9.2	1.9	9.2	1.7	3.3	12.6	0.2	87.1	0.47
M2.01	10.0	10.0	2.0	9.8	1.8	2.8	13.0	0.25	85.6	0.72
M2.02	10.2	9.7	1.6	9.9	1.8	3.6	13.0	0.2	85.2	----
M2.03	11.0	11.0	1.8	10.7	1.6	2.6	13.0	0.3	88.8	----
M2.04	10.6	10.5	2.2	9.9	1.38	2.2	13.0	0.25	89.6	----
M2.05	9.7	9.7	1.8	9.5	1.6	4.0	13.0	0.17	87.8	0.74
M2.06	9.6	9.6	2.2	9.6	2.2	5.2	13.4	0.3	90.2	----
M2.11	7.3	1.0	0.15	3.6	0.5	4.8	13.0	0.15	25.0	2.8
M2.12	5.6	0.06	0.02	0.8	0.36	2.6	13.0	0.2	12.2	4.1
M2.21	14.1	14.1	4.1	13.9	1.86	2.8	12.6	0.24	123.1	0.5
M2.22	13.9	12.4	2.8	13.5	2.2	5.0	13.0	0.31	118.7	0.60
M2.31	8.2	7.8	1.5	8.0	1.2	4.5	13.0	0.22	72.6	0.65
M2.32	9.1	8.2	2.0	8.5	1.2	4.0	13.0	0.18	78.2	0.55
M2.41	9.4	6.9	1.3	8.5	0.8	6.8	12.8	0.18	80.5	----
M2.42	8.6	8.6	2.0	8.6	1.0	3.0	12.8	0.22	77.4	0.65

List of Figures

Fig. 1. Definitions of the studied factors representing confinement conditions
Fig. 2. Idealized bond-slip response envelopes for different concrete confining levels
Fig. 3. Examples of obtained cyclic responses and its schematic representation
Fig. 4. Ratio E_0/E_c versus the confinement Index I_c
Fig. 5. Ratio τ_2/τ_{1c} versus E_0/E_c ratio
Fig. 6. Ratio τ_2/τ_1 versus E_o/E_c ratio
Fig. 7. Ratio τ_3/τ_{3c} versus E_0/E_c ratio
Fig. 8. Proposed model and other models predictions versus a selection of idealized experimental envelope curves obtained in M-Series
Fig. 9. Proposed model and other models predictions versus Harajli et al. (2004) B3N specimen experimental response
Fig.10. Proposed model predictions versus experimental values of Series 1.3 and 1.4 from Eligehausen et al. 1983

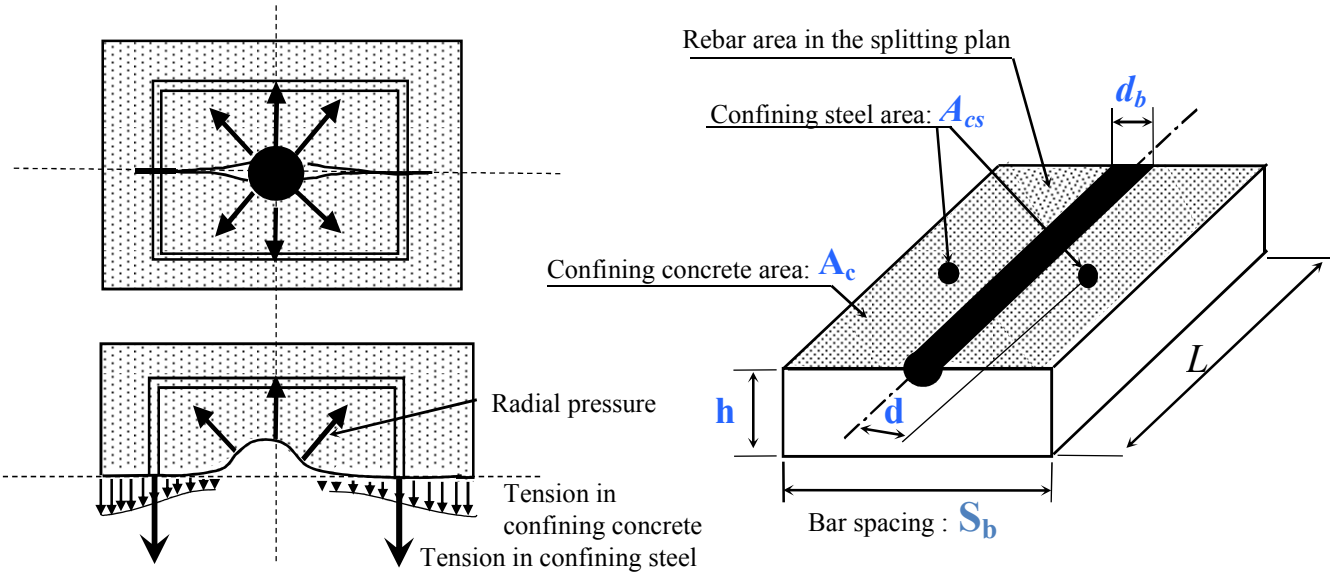
Rebar area in the splitting plan
Confining steel area: A_{cs}
d_b
Confining concrete area: A_c
Radial pressure
Tension in confining concrete
Tension in confining steel
h
d
L
Bar spacing : S_b

Fig. 1

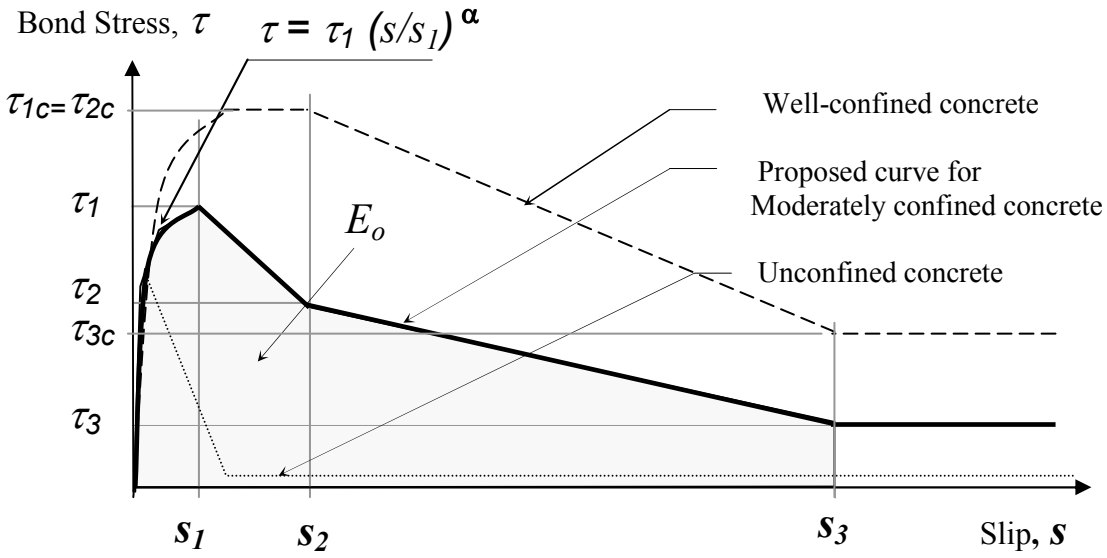
Bond Stress, τ
τ = τ1 (s/s1) α
τ1c= τ2c
τ1
τ2
τ3c
τ3
Eo
Well-confined concrete
Proposed curve for
Moderately confined concrete
Unconfined concrete
s1
s2
s3
Slip, s

Fig. 2

Fig. 1

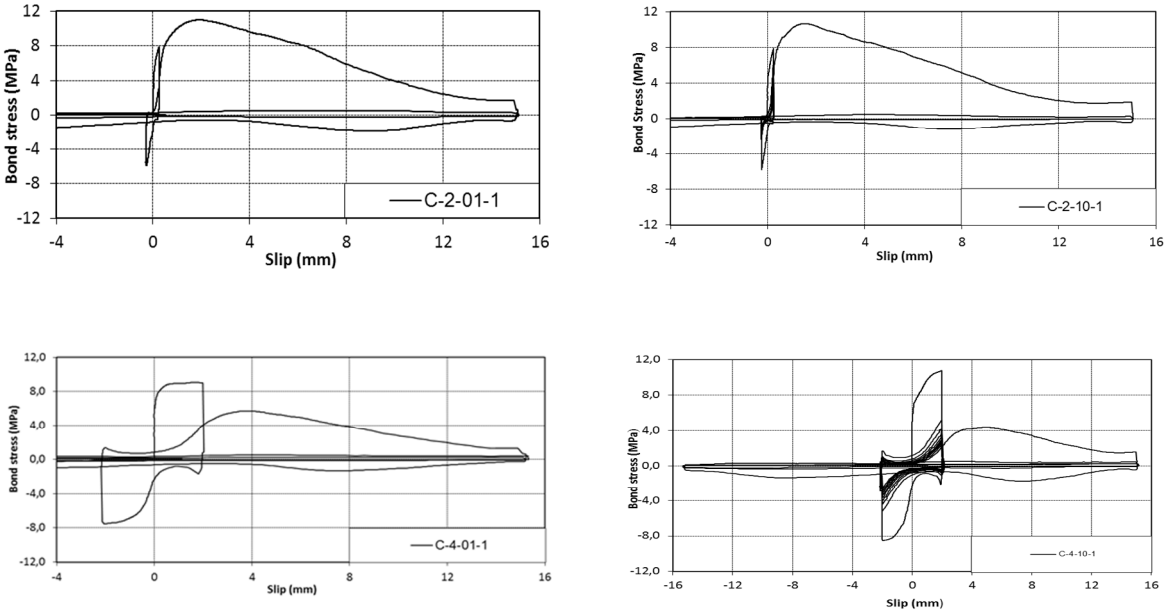
Bond stress (MPa)
Slip (mm)
C-2-01-1
Bond Stress (MPa)
C-2-10-1
C-4-01-1
C-4-10-1

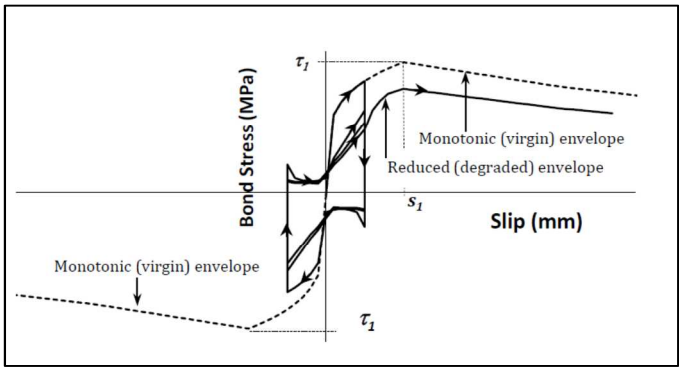
τ_1
Bond Stress (MPa)
Monotonic (virgin) envelope
Reduced (degraded) envelope
s_1
Slip (mm)
Monotonic (virgin) envelope
τ_1

Fig. 3

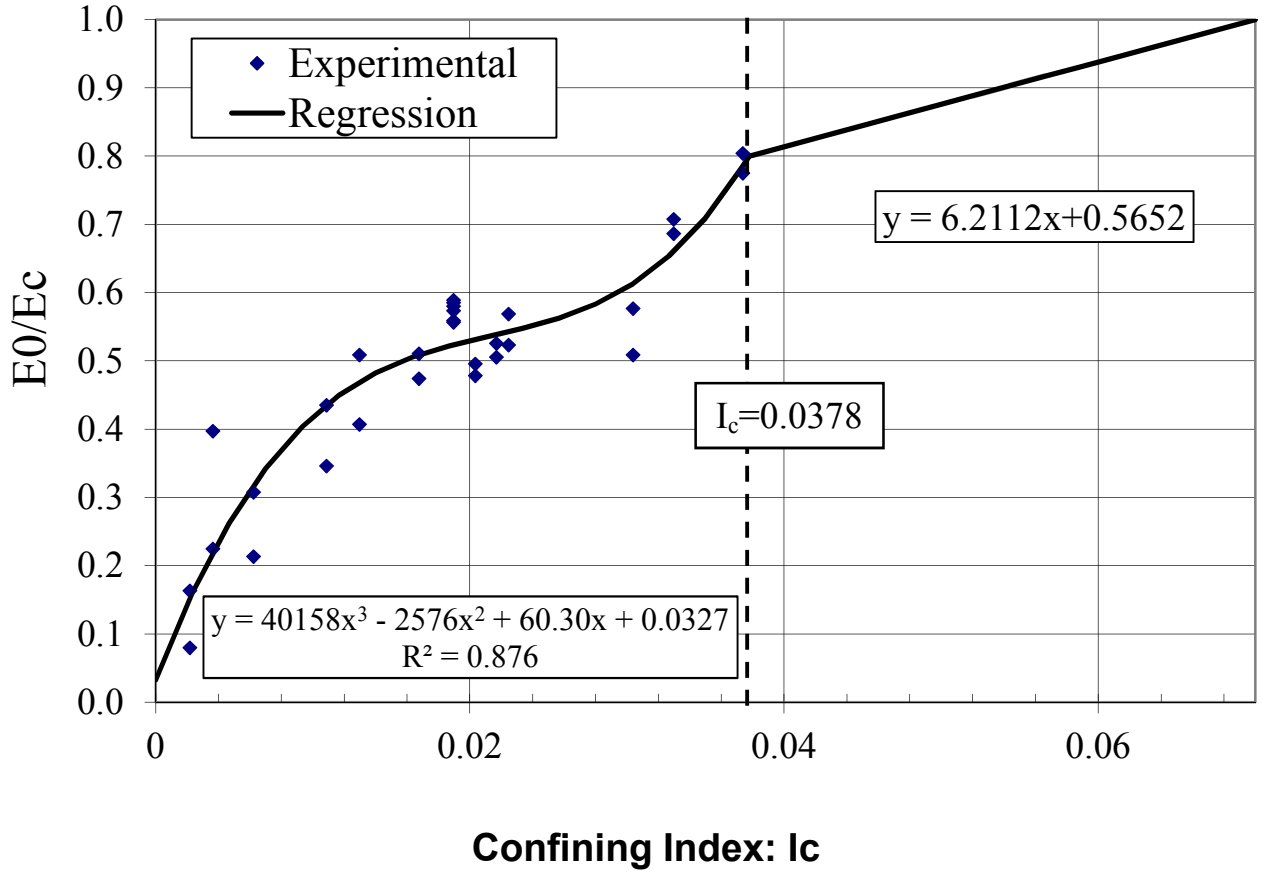
Experimental
Regression
y = 6.2112x+0.5652
I_c=0.0378
y = 40158x³ - 2576x² + 60.30x + 0.0327
R² = 0.876
E0/Ec
Confining Index: Ic
1.0
0.9
0.8
0.7
0.6
0.5
0.4
0.3
0.2
0.1
0.0
0
0.02
0.04
0.06

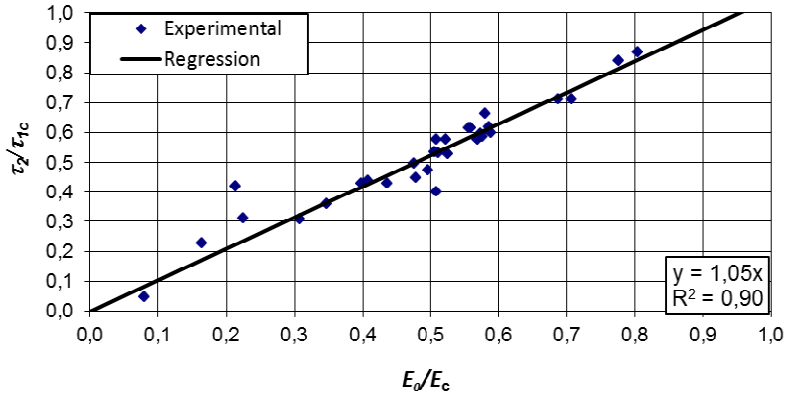
Experimental
Regression
y = 1,05x
R² = 0,90
1,0
0,9
0,8
0,7
0,6
0,5
0,4
0,3
0,2
0,1
0,0
0,0
0,1
0,2
0,3
0,4
0,5
0,6
0,7
0,8
0,9
1,0
τ_2/τ_{1c}
E_d/E_c

Fig. 5

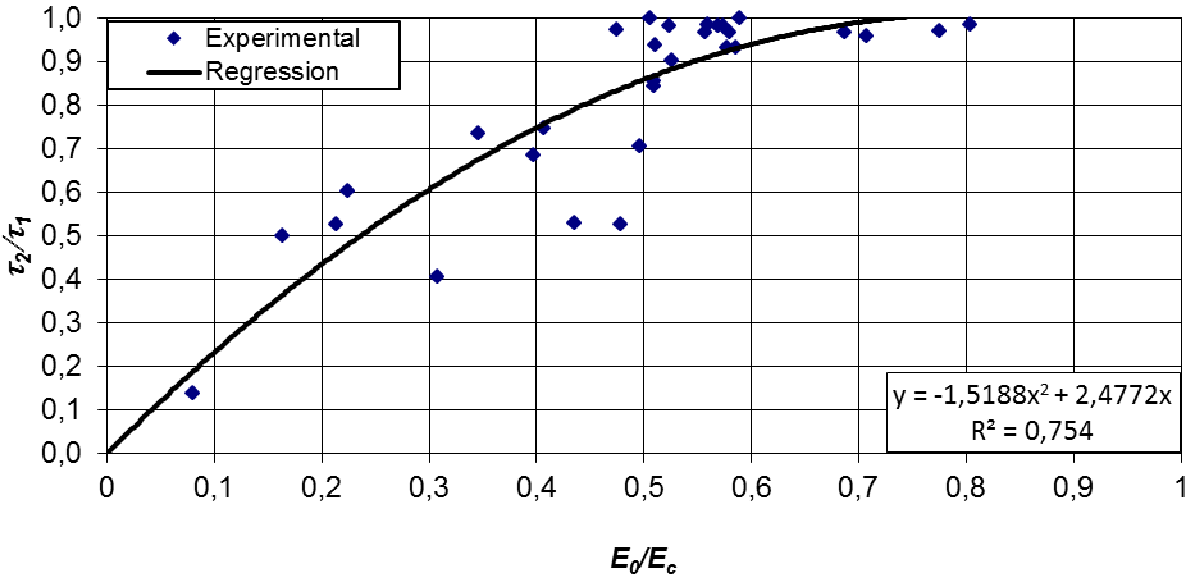
Experimental
Regression
y = -1,5188x² + 2,4772x
R² = 0,754
τ2/τ1
E0/Ec
1,0
0,9
0,8
0,7
0,6
0,5
0,4
0,3
0,2
0,1
0,0
0
0,1
0,2
0,3
0,4
0,5
0,6
0,7
0,8
0,9
1

Fig.6

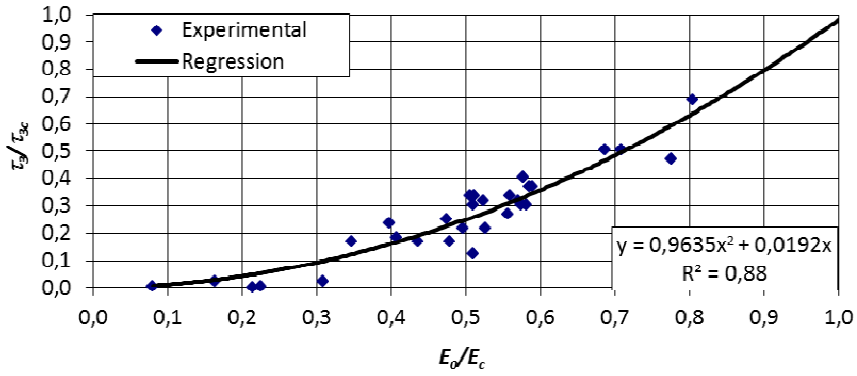
Experimental
Regression
y = 0,9635x² + 0,0192x
R² = 0,88
τ_y/τ_xc
E_o/E_c
1,0
0,9
0,8
0,7
0,6
0,5
0,4
0,3
0,2
0,1
0,0
0,0
0,1
0,2
0,3
0,4
0,5
0,6
0,7
0,8
0,9
1,0

Fig. 7

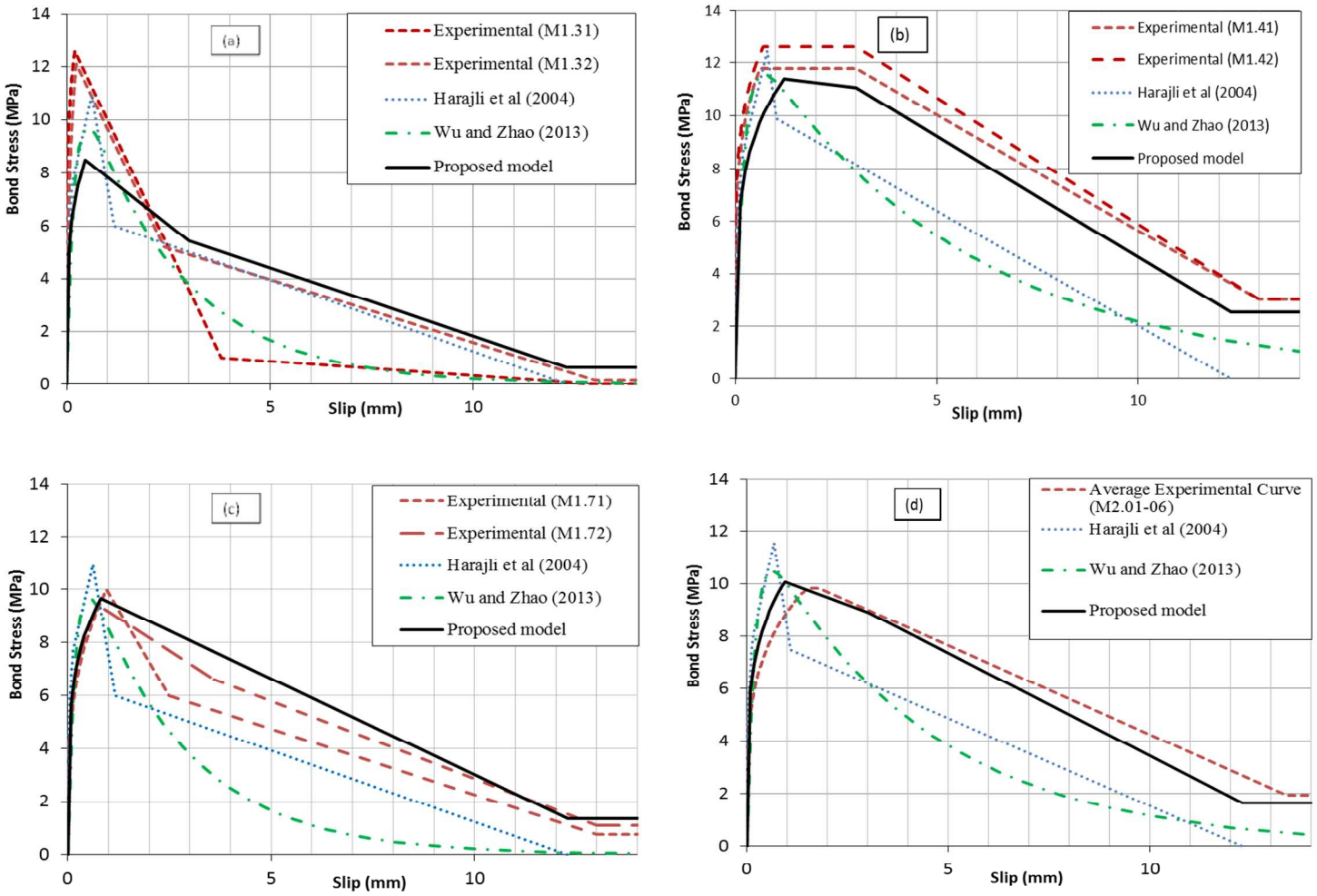
(a)
Experimental (M1.31)
Experimental (M1.32)
Harajli et al (2004)
Wu and Zhao (2013)
Proposed model
Bond Stress (MPa)
Slip (mm)
(b)
Experimental (M1.41)
Experimental (M1.42)
Harajli et al (2004)
Wu and Zhao (2013)
Proposed model
Bond Stress (MPa)
Slip (mm)
(c)
Experimental (M1.71)
Experimental (M1.72)
Harajli et al (2004)
Wu and Zhao (2013)
Proposed model
Bond Stress (MPa)
Slip (mm)
(d)
Average Experimental Curve (M2.01-06)
Harajli et al (2004)
Wu and Zhao (2013)
Proposed model
Bond Stress (MPa)
Slip (mm)

Fig. 8

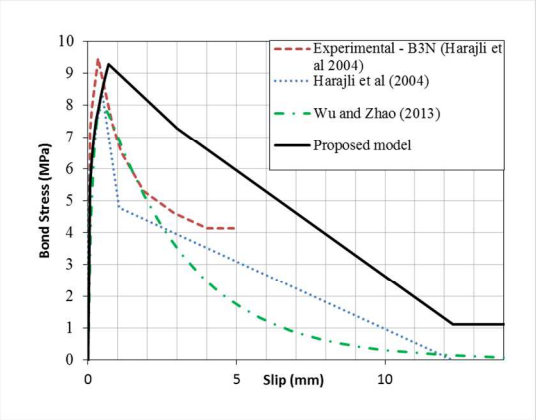
Experimental - B3N (Harajli et al 2004)
Harajli et al (2004)
Wu and Zhao (2013)
Proposed model
Bond Stress (MPa)
Slip (mm)
0
1
2
3
4
5
6
7
8
9
10
0
5
10

Fig. 9

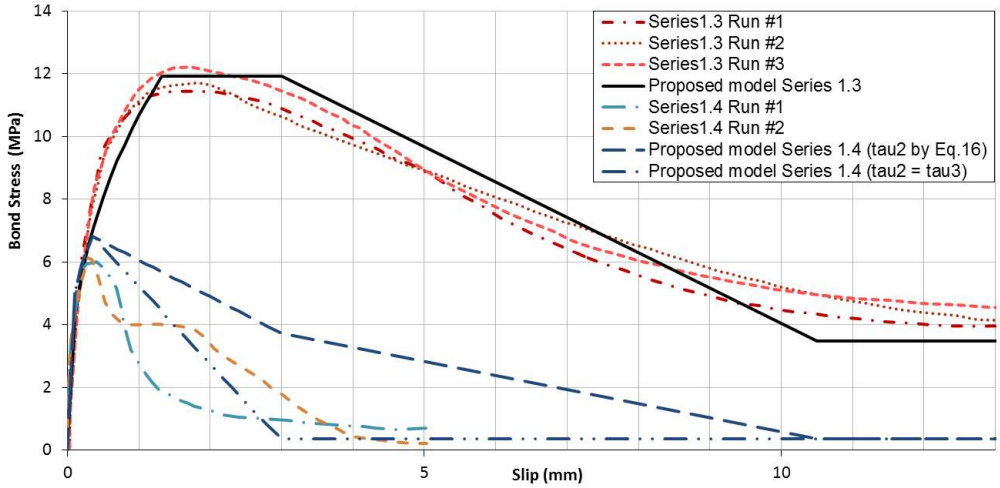
Bond Stress (MPa)
Slip (mm)
0
2
4
6
8
10
12
14
0
5
10
Series1.3 Run #1
Series1.3 Run #2
Series1.3 Run #3
Proposed model Series 1.3
Series1.4 Run #1
Series1.4 Run #2
Proposed model Series 1.4 (tau2 by Eq.16)
Proposed model Series 1.4 (tau2 = tau3)

Fig. 10